

The FRUITY database on AGB stars: past, present and future

Sergio Cristallo

INAF Osservatorio Astronomico di Teramo, via Maggini sn 64100 - Teramo (Italy)
INFN Sezione Napoli, Napoli (Italy)

E-mail: cristallo@oa-teramo.inaf.it

Luciano Piersanti

INAF Osservatorio Astronomico di Teramo, via Maggini sn 64100 - Teramo (Italy)
INFN Sezione Napoli, Napoli (Italy)

Oscar Straniero

INAF Osservatorio Astronomico di Teramo, via Maggini sn 64100 - Teramo (Italy)
INFN Sezione Napoli, Napoli (Italy)

Abstract. We present and show the features of the FRUITY database, an interactive web-based interface devoted to the nucleosynthesis in AGB stars. We describe the current available set of AGB models (largely expanded with respect to the original one) with masses in the range $1.3 \leq M/M_{\odot} \leq 3.0$ and metallicities $-2.15 \leq [\text{Fe}/\text{H}] \leq +0.15$. We illustrate the details of our s-process surface distributions and we compare our results to observations. Moreover, we introduce a new set of models where the effects of rotation are taken into account. Finally, we shortly describe next planned upgrades.

1. Introduction

Asymptotic Giant Branch stars (hereafter AGBs) are exceptional laboratories to test the robustness of stellar models. During this evolutionary phase, both light (C, N, F, Na) and heavy elements can be produced. The latter are synthesized via the slow neutron capture process (the s-process). A detail description of AGBs evolution and nucleosynthesis can be found in [1].

The structure of an AGB consists of a partially degenerate CO core, surrounded by an He-shell and an H-shell separated by a thin layer (He-intershell) and by a cool and expanded convective envelope. The surface luminosity is mainly sustained by the H-burning shell, active for most of the time. This situation is recurrently interrupted by the growing up of thermonuclear runaways driven by violent ignitions of 3α reactions at the base of the He-intershell (Thermal Pulses, hereafter TPs). The energy suddenly released by TPs can not be transported outward radiatively and, thus, convective episodes develop. These convective shells efficiently mix the He-intershell, enriching this layer in carbon (produced by 3α reactions) and in s-process elements. Moreover, the energy boosted by the TP forces the overlying layers to expand, possibly switching off the H-shell. This allows the convective envelope to penetrate downward, carrying to the surface the

F.R.U.I.T.Y.
(FULL-Network Repository of Updated Isotopic Tables & Yields)

Select Data:

Mass (M_{\odot})	Metallicity (Z) ⁽¹⁾	Nuclides Properties	Multiple Table format ⁽⁸⁾	Single Table format ⁽⁹⁾
---	---	<input type="radio"/> Elements ^(2,3) Z: All <input type="radio"/> Isotopes ⁽⁴⁾ A: All Z: All <input type="radio"/> s-process ⁽⁶⁾ : [hs/ls], [Pb/hs], ... <input type="radio"/> Net ⁽⁷⁾ <input type="radio"/> Yields ⁽⁶⁾ A: All Z: All <input type="radio"/> Total	<input type="radio"/> All Dredge Up Episodes ⁽¹⁰⁾ <input type="radio"/> Final Composition <input type="radio"/> Final	<input type="radio"/> Final Composition <input type="radio"/> Final

☐ Don't Show / Only files

[NOTES ON THE MODELS \(pdf file\)](#)

Figure 1. The FRUITY database homepage.

isotopes freshly synthesized in the He-intershell. This phenomenon is called Third Dredge Up (hereafter TDU) and it is known to work in AGB stars since the early fifties [2].

The major neutron source in AGB stars is the $^{13}\text{C}(\alpha, n)^{16}\text{O}$ reaction. Neutrons are released within the He-intershell during the interpulse phase (thus in radiative conditions) when $T \sim 1.0 \times 10^8$ K [3]. Actually, the amount of ^{13}C requested to fit observations is one of the major sources of uncertainty in AGB models ([4]; see also Section 2). A marginal contribution comes from the $^{22}\text{Ne}(\alpha, n)^{25}\text{Mg}$ reaction, which is activated at higher temperatures ($T > 2.5 \times 10^8$ K) during TPs.

The great amount of available spectroscopic data such as the need of yields for Chemical Evolution Models require the computation of a large number of detailed AGB evolutionary models. We fit this request by making available our theoretical results on the on-line web pages of the FRUITY (FUNs Repository of Updated Isotopic Tables & Yields) database, entirely dedicated to the nucleosynthesis in AGB stars.

In Section 2 we briefly present our evolutionary code (FUNs), while in Section 3 we describe the set of models currently available on FRUITY. In Section 5 we present a recently published set of rotating AGB stars. Finally, in Section 6 we list our planned upgrades.

2. The FUNs evolutionary code

The FUNs (Full Network stellar) evolutionary code is a one-dimension hydrostatic code (see [1] and references therein). The adopted mass-loss rate has been calibrated on the Period-Luminosity and Period-Mass loss relations observed in Long Period Variable Stars [1]. In the envelope, atomic and molecular opacities are calculated according to the changes in the chemical composition due to the occurrence of TDU episodes [4]. The radiation/convection interface at the inner border of the convective envelope is treated by applying an exponential decay of the convective velocities. As a by-product, we obtain the self-consistent formation of the ^{13}C pocket after each TP followed by TDU. The extension of the that pocket varies from TP to TP following

the shrinking of the He-intershell [5]. In order to avoid the possible loss of accuracy inherent to post-process techniques, we directly coupled our models to a full nuclear network, which includes all isotopes from hydrogen to bismuth (at the ending-point of the s-process path).

3. The FRUITY database

The original set of FRUITY has been presented in [6]. It consists of 28 evolutionary models, with different combinations of masses (1.5, 2.0, 2.5, and 3.0 M_{\odot}) and metallicities ($[\text{Fe}/\text{H}] = -1.15, -0.67, -0.37, -0.24, -0.15, 0.00, +0.15$). Different He contents and scaled solar compositions [7] are used (see [6] for details).

Recently, new models have been uploaded. In particular, the mass range has been expanded down to 1.3 M_{\odot} models. Note that, at large metallicities, these masses do not experience TDU episodes.

In order to cover the metallicity range of Galactic Globular Clusters, we compute two additional metallicities: $[\text{Fe}/\text{H}] = -2.15$ and $[\text{Fe}/\text{H}] = -1.67$, both of them with α -enhanced elements ($[\alpha/\text{Fe}] = 0.5$).

For each model, users can freely download pulse by pulse surface isotopic compositions and elemental overabundances¹. Tables are available in two different formats (see Figure 1). In the Multiple Table Format, the query returns multiple table, depending on the number of selected models. In the Single Table Format, the query returns a single table containing all the selected models; in this case, only single elements (or isotopes) can be visualized. Among other quantities available on FRUITY there are the $[\text{ls}/\text{Fe}]$ ², the $[\text{hs}/\text{Fe}]$ ³ and the s-process indexes $[\text{hs}/\text{ls}]$, $[\text{Pb}/\text{hs}]$ and $[\text{Pb}/\text{ls}]$. Finally, stellar yields can be selected. With respect to the original version of the FRUITY database, beside net yields we also made available total stellar yields.

Users interested in upgrades of the FRUITY database can register to the dedicated mailing list.

4. Comparison to observations

In order to verify the robustness of our models, we compare them to their observational counterparts. In particular, we concentrate on the Luminosity Function of Carbon Stars (hereafter LFCS) and on s-process spectroscopic indexes at different metallicities.

The LFCS links the luminosity of these objects (and thus the core mass; see [8]) with their carbon surface abundance. Thus, by studying this quantity, we can test our prescriptions on convection and mass-loss law. In 2006, [9] analyzed a sample of Galactic Carbon Stars and show how the radiation emitted by these objects at infrared wavelengths strongly weights the LFCS toward large λ . Recently, [10] proposed a re-analysis of the same sample and found that the high luminosity tail of the LFCS described by [9] disappears, in good agreement with theoretical expectations [6].

Another useful litmus test for theoretical models is the study of s-process spectroscopic indexes, in particular the $[\text{hs}/\text{ls}]$ and the $[\text{Pb}/\text{hs}]$. Before introducing them, a distinction between intrinsic and extrinsic s-process rich stars has to be done.

TP-AGB stars are intrinsic s-rich stars, since they are presently undergoing thermal pulses and TDU episodes. Post-AGB stars belong to the same class.

Extrinsic s-rich stars are less-evolved stars (dwarfs or giants) belonging to binary systems, whose s-enhancement is likely due to the pollution caused by the intense wind of an AGB companion. Ba-stars and, at lower metallicities, CH stars and Carbon Enhanced Metal Poor s-process rich stars (hereafter CEMP-s stars) belong to this class of objects.

The only possibility to group together all s-rich stars is to study relative surface abundances. In

¹ In the usual spectroscopic notation: $[\text{El}/\text{Fe}] = \log(\text{N}(\text{El})/\text{N}(\text{Fe}))_{*} - \log(\text{N}(\text{El})/\text{N}(\text{Fe}))_{\odot}$

² $[\text{ls}/\text{Fe}] = ([\text{Sr}/\text{Fe}] + [\text{Y}/\text{Fe}] + [\text{Zr}/\text{Fe}])/3$

³ $[\text{hs}/\text{Fe}] = ([\text{Ba}/\text{Fe}] + [\text{La}/\text{Fe}] + [\text{Nd}/\text{Fe}] + [\text{Sm}/\text{Fe}])/4$

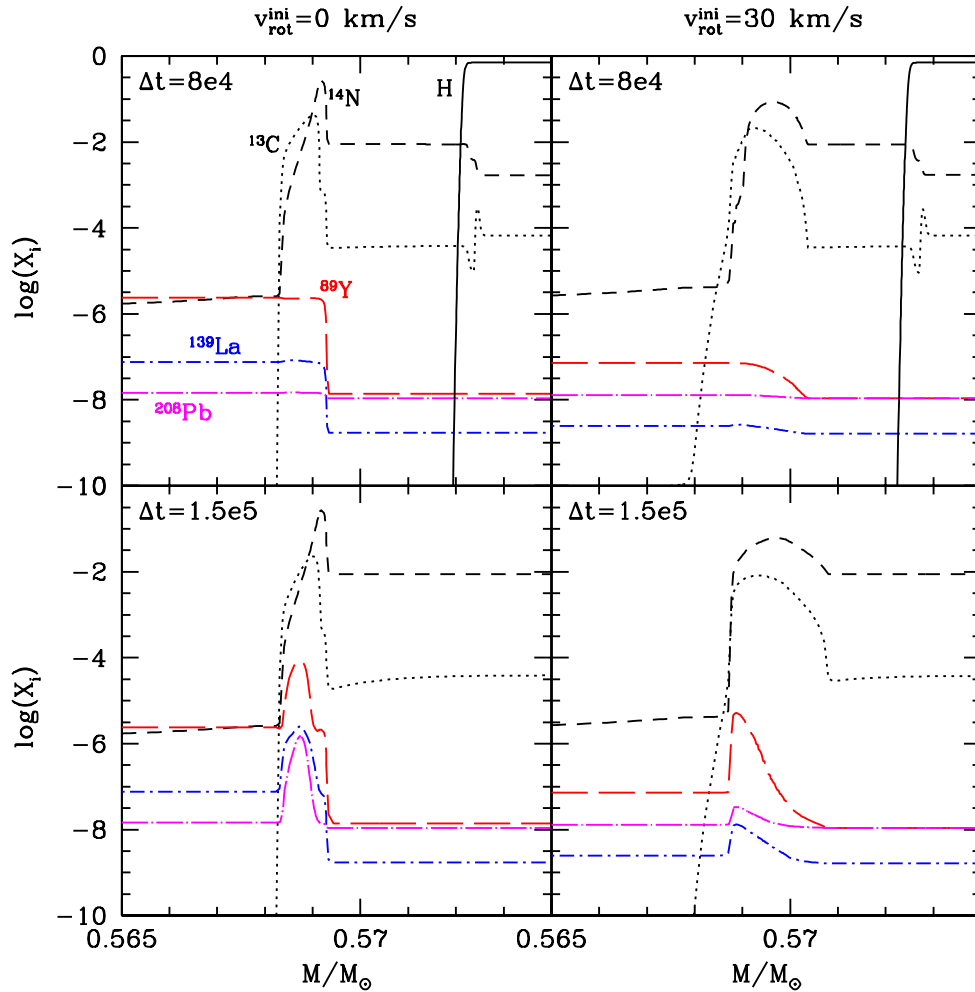


Figure 2. Temporal evolution of key elements during the radiative burning of the 2nd ^{13}C pocket of a $2 M_{\odot}$ star with $Z=10^{-2}$ and different initial rotation velocities. See text for details.

such a way, any problem correlated to possible further dilution process or to their evolutionary status is avoided.

We have already shown that our theoretical models match observations, even if they are not able to explain the observed spread for a fixed metallicity (see Fig. 12 and 13 of [6]). Although it is possible that (at least part of) the observed spread can be ascribed to the large observational uncertainties, theoretical scenarios able to explain such a spread has to be explored. Among them, we verified is the mixing induces by rotation can lead to a certain spread of the spectroscopic indexes.

5. Low mass rotating AGB models

Even if low mass stars are generally slow rotators, the lifting due to the centrifugal force and the mixing induced by dynamical and secular instabilities can modify their physical structure and chemical composition. In order to verify the effect that rotation can have on the nucleosynthesis during the AGB phase, we implement our models with rotation. In particular, we add rotation-

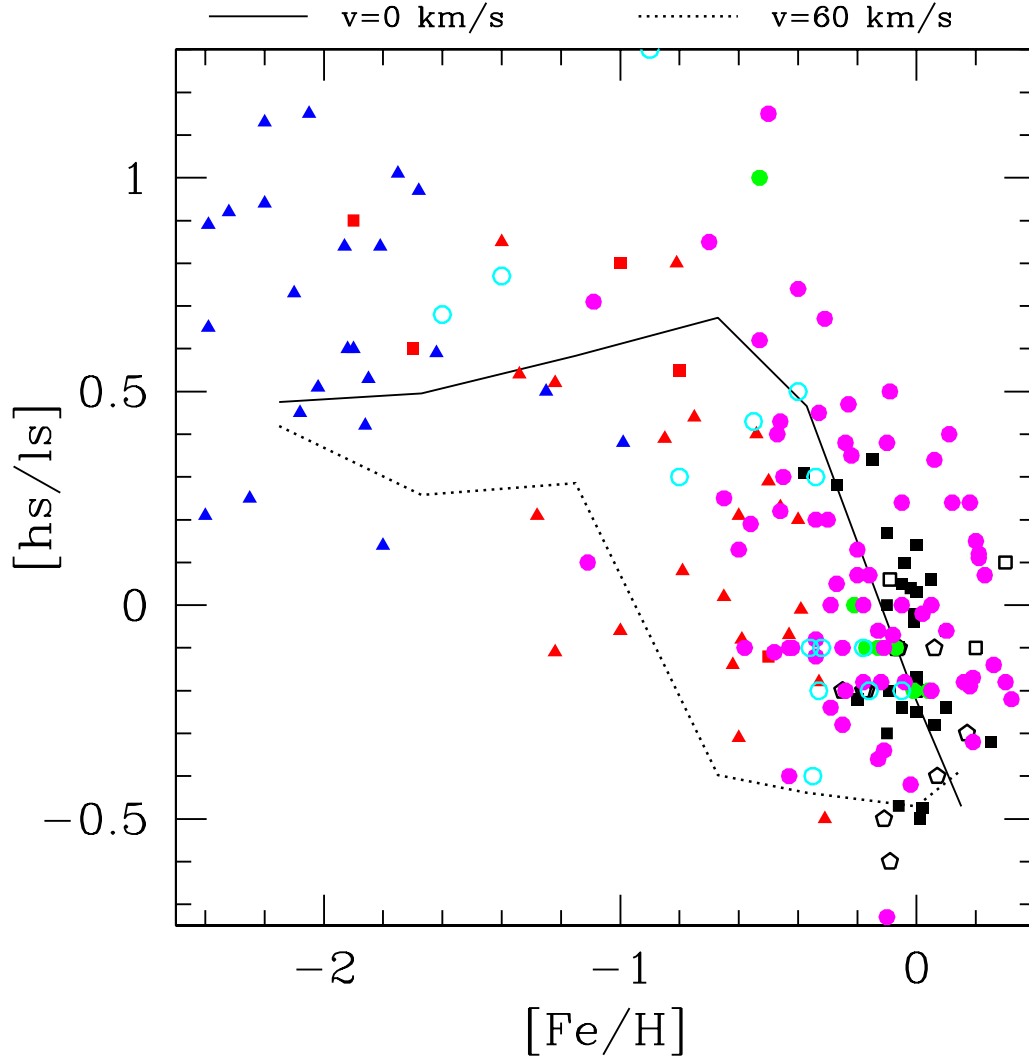


Figure 3. $[hs/ls]$ s-process index as a function of metallicity for models with and without rotation. See text for details.

induced mixing to the other mixing already considered in our previous works, those due to convection in particular. We found that a variation in the initial velocity can lead to a consistent spread in the final surface s-process enhancements and spectroscopic indexes for stars with the same initial mass and metallicity [11].

Rotation does not determine the formation of the ^{13}C pocket. Notwithstanding, rotation-induced mixing modify the mass extension of both the ^{13}C and the ^{14}N pockets and their overlap, thus reducing the average neutrons-to-seeds ratio. In Figure 2 we report the ^{13}C and the ^{14}N abundances in the region where the 2nd ^{13}C pocket of a $2 M_{\odot}$ star with $Z=10^{-2}$ forms. Left panels refer to a non-rotating model, while right panels to a model with initial rotation velocity $v_{rot}^{ini}=30$ km/s . In the same plot we also report the local abundances of ^{89}Y , ^{139}La and ^{208}Pb , assumed as representative of the three s-process peaks. We find that the Goldreich-Schubert-Fricke instability, active at the interface between the convective envelope and the rapid rotating core, contaminates the ^{13}C -pocket with ^{14}N . Thus, the mixing induced by rotation locally decreases the neutron-to-seed ratio, leading to a reduction of the total amount of heavy elements

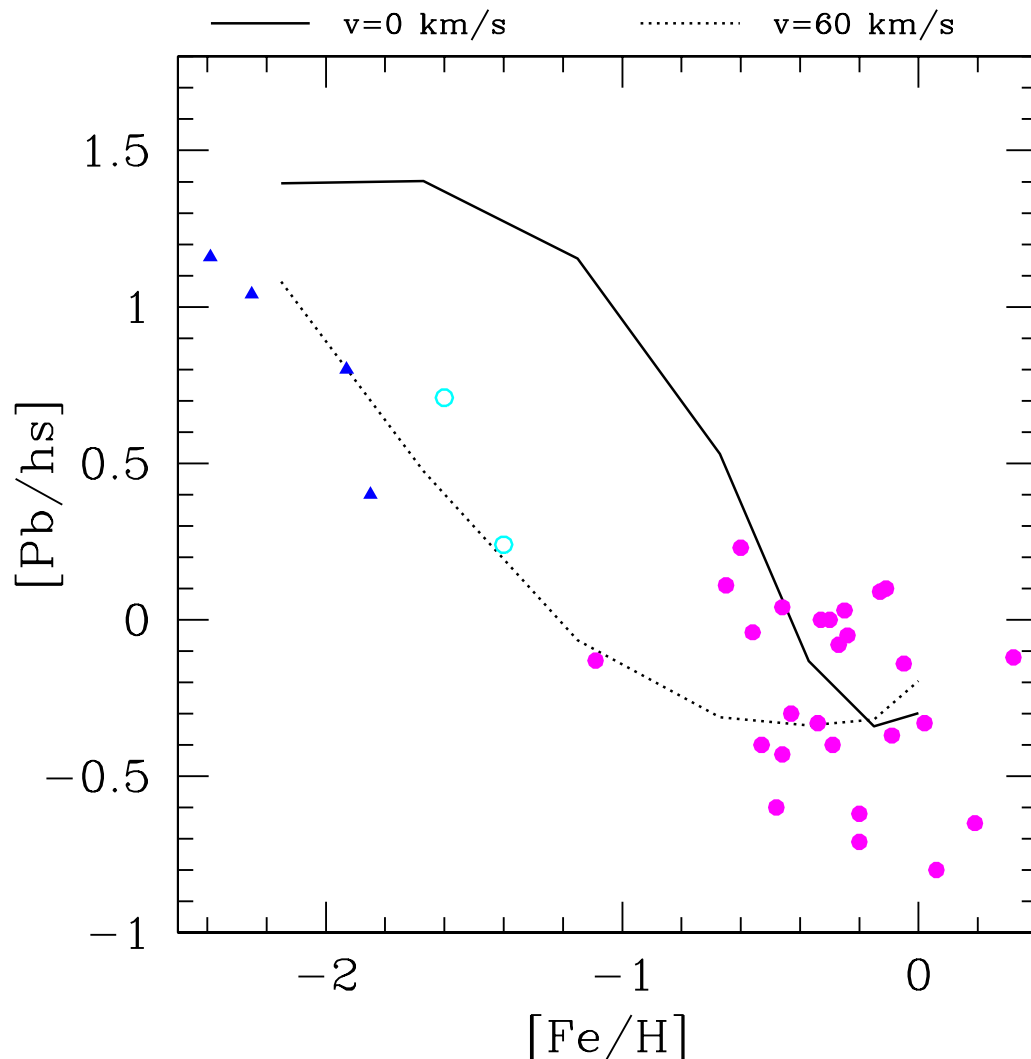


Figure 4. As in Figure 3, but for the $[\text{Pb}/\text{hs}]$ s-process index.

produced by the s process and favoring the light-s elements with respect to the heavier ones. As a matter of fact, both the $[\text{hs}/\text{ls}]$ and the $[\text{Pb}/\text{hs}]$ spectroscopic indexes decrease as the initial rotation velocity increases (see Figures 6 and 9 of [11]). At low metallicity, the combined effect of Goldreich-Schubert-Fricke instability and meridional circulations determines an increase of light-s and, to a less extent, heavy-s elements, while lead is strongly reduced.

In Figures 3 and 4 we report, as a function of the metallicity, the $[\text{hs}/\text{ls}]$ and $[\text{Pb}/\text{hs}]$ s-process indexes for models with and without rotation. Two values of initial rotation velocities ($v_{\text{rot}}^{\text{ini}}=60$ km/s and $v_{\text{rot}}^{\text{ini}}=120$ km/s) have been considered. With respect to the observational data reported in [6], we add recent measurements of post-AGB stars [12,13,14,15], Ba-stars [16,17], CH stars [18,19,20] and a selection of well measured CEMP-s stars (see [21] and references therein).

Our results suggest that rotation can be regarded as a possible physical mechanism responsible for the observed spread of s-process spectroscopic indexes. In particular, the large spread in the $[\text{hs}/\text{ls}]$ at intermediate metallicities ($-1.0 < [\text{Fe}/\text{H}] < -0.6$) can be reproduced by hypothesizing different initial rotation velocities. Notwithstanding, our models cannot match the large $[\text{hs}/\text{ls}]$ (up to 1) measured at low metallicities. Interestingly, the lower $[\text{Pb}/\text{hs}]$ values characterizing

rotating models are in agreement with observations. In fact, as shown in Figure 4, models with $v_{rot}^{ini}=60$ km/s better reproduce the sequence, starting from high Z, of Ba-stars (full dots), CH stars (open dots) and CEMP-s stars (full triangles). Unfortunately, firm conclusions cannot be drawn due to the paucity of lead measurements and to the large errors affecting observations.

6. Planned Upgrades

The current version of FRUITY spans on a reasonable range of metallicities and well covers the low mass range. Intermediate mass AGB stars ($4 < M/M_{\odot} < 7$; hereafter IM-AGBs) are currently missing. These stars are particularly important for the chemical evolution of Globular Clusters (see e.g. [22] and references therein). We already conducted an explorative study of IM-AGBs [23], but without publishing detailed nucleosynthetic predictions. Therefore, we intend to explore the evolution and nucleosynthesis of IM-AGBs, starting from the metallicities of interest for the study of Galactic Globular Clusters [24]. Later, we aim to extend these calculations to all the metallicities considered in FRUITY.

Finally, as a long-term project, we are planning to extend the mass range of FRUITY to massive stars, in order to study the weak component of the s-process, at work during the core-He burning and the C-burning shell phases particularly efficient when rotation is explicitly taken into account. (see [25] and references therein).

6.1. Acknowledgments

The authors warmly thank Prof. Roberto Gallino for continuous and fruitful scientific discussions.

7. References

- [1] Straniero O, Gallino R and Cristallo S 2006 *Nucl. Phys. A* **777** 311
- [2] Merrill P W 1952 *Astrophys. J.* **116** 21
- [3] Straniero O, Gallino R, Busso M, Chieffi A, Limongi M & Salaris M 1995 *Astrophys. J. Lett.* **440** 85
- [4] Gallino R, Arlandini C, Busso M, Lugaro M, Travaglio C, Straniero O, Chieffi A and Limongi M 1998 *Astrophys. J.* **497** 388
- [5] Cristallo S, Straniero O, Lederer M T and Aringer B 2007 *Astrophys. J.* **667** 489
- [6] Cristallo S, Piersanti L, Straniero O, Gallino R, Dominguez I, Abia C, Di Rico G, Quintini M and Bisterzo S 2011 *Astrophys. J. Suppl.* **197** 17
- [7] Lodders K 2003 *Astrophys. J.* **591** 1220
- [8] Paczynski B 1970 *Acta Astron.* **20** 47
- [9] Guandalini R, Busso M, Ciprini S and Silvestro G 2006 *Astron. & Astrophys.* **445** 1069
- [10] Guandalini R and Cristallo S 2013 *Astron. & Astrophys.* **555** 120
- [11] Piersanti L, Cristallo S and Straniero O 2013 *Astrophys. J. accepted* (arXiv1307.2017)
- [12] Sumangala Rao S, Pandey G, Lambert D L and Giridhar S 2011 *Astrophys. J. Lett.* **737** 7
- [13] Pereira C B, Gallino R and Bisterzo S 2012 *Astron. & Astrophys.* **538** 48
- [14] De Smedt K, Van Winckel H, Karakas A I, Siess L, Goriely S and Wood P R 2012 *Astron. & Astrophys.* **541** 67
- [15] van Aarle E, Van Winckel H, De Smedt K, Kamath D and Wood P R 2013 *Astron. & Astrophys.* **554** 106
- [16] Pereira C B, Sales Silva J V, Chavero C, Roig F and Jilinski E 2011 *Astron. & Astrophys.* **533** 51
- [17] Lebzelter T, Uttenthaler S, Straniero O and Aringer B 2013 *Astron. & Astrophys.* **554** 30
- [18] Pereira C B and Drake N A 2011 *Astron. Journ.* **141** 79
- [19] Pereira C B, Jilinski E, Drake N A, de Castro D B, Ortega V G, Chavero C and Roig F 2012 *Astron. & Astrophys.* **543** 58
- [20] Liu S, Nissen P E, Schuster W J, Zhao G, Chen Y Q and Liang Y C 2012 *Astron. & Astrophys.* **541** 88
- [21] Bisterzo S, Gallino R, Straniero O, Cristallo S and Kappeler F 2012 *MNRAS* **422** 849
- [22] Ventura P and D’Antona F 2009 *Astron. & Astrophys.* **402** 72
- [23] Straniero O, Limongi M, Chieffi A, Dominguez I, Busso M and Gallino R 2000 *MemSAIt* **71** 719
- [24] Straniero O, Cristallo S and Piersanti L 2013 *MemSAIt* **84** 105
- [25] Pignatari M, Gallino R, Meynet G, Hirschi R, Herwig F and Wiescher M 2008 *Astrophys. J. Lett.* **687** 95